

Porphyrin Assemblies on DNA as Studied by a Resonance Light-Scattering Technique

Robert F. Pasternack,^{*,†} Carlos Bustamante,[‡] Peter J. Collings,[§] Antonino Giannetto,[†] and Esther J. Gibbs[⊥]

Contribution from the Department of Chemistry and Department of Physics and Astronomy, Swarthmore College, Swarthmore, Pennsylvania 19081

Received February 23, 1993

Abstract: Under appropriate conditions of concentration and ionic strength, *trans*-bis(*N*-methylpyridinium-4-yl)-diphenylporphine and its copper(II) derivative produce very large, bisignate circular dichroism signals in the Soret region when bound to DNA. The processes leading to these signals are shown to be highly cooperative. A new light-scattering experimental approach is described for detecting such extended aggregates of chromophores in which the radiation used is within an absorption maximum, specifically in the porphyrin Soret absorption region. Results from such resonance light-scattering experiments confirm that extended porphyrin aggregates form on the DNA, which, in contrast, remains dispersed. A model for these interactions consistent with experimental findings involves porphyrin organization into long-range chiral structures having antenna-like properties, that is, forming assemblies in which the electric field produced in one oscillating dipole affects the magnitude of (is coupled to) the other dipoles in the aggregate.

Introduction

Cationic meso-substituted porphyrins and their metalloderivatives are proving valuable as probes of nucleic acid structure and dynamics.¹ The observation of (rapid²) uptake³ of porphyrins by DNA has helped form the basis for a proposal for a "quake" (collective motion) model for nucleic acids, involving the simultaneous breaking of multiple adjacent hydrogen bonds;⁴ porphyrins have been shown to be capable of interacting with Z-DNA and converting it to the B-form;^{5,6} energy-transfer processes through the double helix have been investigated with porphyrin acceptors;⁷ and several derivatives have been reported as showing nuclease activity, making them useful reagents for footprinting experiments.⁸⁻¹⁰

Among the advantages synthetic cationic porphyrins (and metalloporphyrins) offer as model drugs and probes are the following: (i) a number of these species are quite water-soluble, and their solution chemistry has been extensively studied; (ii) they are intense chromophores and many fluoresce, providing convenient signals for monitoring reactions; (iii) they are readily derivatized, permitting systematic studies of the probe's interactions with nucleic acids; and (iv) the majority of these cationic porphyrins do not aggregate extensively, simplifying analysis.

Based upon studies with such porphyrins, we have proposed^{11,12} that at low levels of drug load, the sign of the induced circular dichroism (CD) spectrum in the Soret region can be used as a signature for the binding mode to DNA: a positive induced CD band is indicative of external (minor) groove binding, and a negative induced CD band is produced upon intercalation.

Recently we have reported¹³⁻¹⁵ on the solution and DNA-binding properties of two mixed-periphery meso-substituted porphyrins, *cis*- and *trans*-bis(*N*-methylpyridinium-4-yl)diphenylporphine (*c*- and *t*-H₂Pagg, Figure 1). Unlike the porphyrins described above, these derivatives (especially the *trans*), under appropriate conditions of concentration and ionic strength, aggregate extensively in water and bind to both condensed and noncondensed DNA or helical polypeptides¹⁶ to produce intense bisignate circular dichroism spectra whose profile reveals the helical sense of the biopolymer. We have suggested that these large, induced CD signals are signatures for the formation of long-range, organized porphyrin assemblies on the biopolymer, which serves as a template. The driving force for assembly formation is proposed to arise from the tendency for these porphyrins to form stacking-type aggregates, a property which can be tuned and modified by periphery modification¹⁷ or metal substitution.¹⁵ For example, whereas *t*-CuPagg aggregates extensively as does the free-base form of this porphyrin, *t*-AuPagg remains monomeric in solution over the conditions considered. The present study reports on the dependence of assembly formation on solution conditions and examines whether porphyrin aggregation has an impact on the state of the nucleic acid to which it is bound. In particular, as we have shown earlier,¹³ the CD spectrum of the nucleic acid is relatively unperturbed by the

[†] Department of Chemistry, Swarthmore College.

[‡] Present address: Institute of Molecular Biology, University of Oregon, Eugene, OR 97403.

[§] Department of Physics and Astronomy, Swarthmore College.

[⊥] Present address: Dept. of Chemistry, Goucher College, Towson, MD 21204.

(1) Pasternack, R. F.; Gibbs, E. J. *ACS Symp. Ser.* **1989**, *402*, 59.

(2) Pasternack, R. F.; Gibbs, E. J.; Villafranca, J. J. *Biochemistry* **1983**, *22*, 5409.

(3) Fiel, R. J.; Howard, J. C.; Mark, E. H.; Datta-Gupta, N. *Nucleic Acids Res.* **1979**, *6*, 3093.

(4) Chou, K. C.; Mao, B. *Biopolymers* **1988**, *27*, 1795.

(5) Pasternack, R. F.; Sidney, D.; Hunt, P. A.; Snowden, E. A.; Gibbs, E. J. *Nucl. Acids Res.* **1986**, *14*, 3927.

(6) McKinnie, R. E.; Choi, J. D.; Bell, J. W.; Gibbs, E. J.; Pasternack, R. F. *J. Inorg. Biochem.* **1988**, *32*, 207.

(7) Pasternack, R. F.; Caccam, M.; Keogh, B.; Stephenson, T. A.; Williams, A. P.; Gibbs, E. J. *J. Am. Chem. Soc.* **1991**, *113*, 7799.

(8) Fiel, R. J.; Beerman, T. A.; Mark, E. H.; Datta-Gupta, N.; *Biochem. Biophys. Res. Commun.* **1982**, *107*, 1067.

(9) Dabrowiak, J. C.; Ward, B.; Goodisman, J. *Biochemistry* **1989**, *28*, 3314.

(10) Bernadou, J.; Pratiel, G.; Bennis, F.; Girardet, M.; Meunier, B. *Biochemistry* **1989**, *28*, 7268.

(11) Pasternack, R. F.; Gibbs, E. J.; Villafranca, J. J. *Biochemistry* **1983**, *22*, 2406.

(12) Pasternack, R. F.; Garrity, P.; Ehrlich, B.; Davis, C. B.; Gibbs, E. J.; Orloff, G.; Giartosio, A.; Turano, C. *Nucleic Acids Res.* **1986**, *14*, 5919.

(13) Gibbs, E. J.; Tinoco, I., Jr.; Maestre, M. F.; Ellinas, P. A.; Pasternack, R. F. *Biochem. Biophys. Res. Commun.* **1988**, *157*, 350.

(14) Pasternack, R. F.; Brigandi, R. A.; Abrams, M. J.; Williams, A. P.; Gibbs, E. J. *Inorg. Chem.* **1990**, *29*, 4483.

(15) Pasternack, R. F.; Giannetto, A.; Pagano, P.; Gibbs, E. J. *J. Am. Chem. Soc.* **1991**, *113*, 7799.

(16) Pasternack, R. F.; Gibbs, E. J. *J. Inorg. Organomet. Polym.* **1993**, *3*, 77.

(17) Marzilli, L. G.; Petho, G.; Lin, M.; Kim, M. S.; Dixon, D. W. *J. Am. Chem. Soc.* **1992**, *114*, 7575.

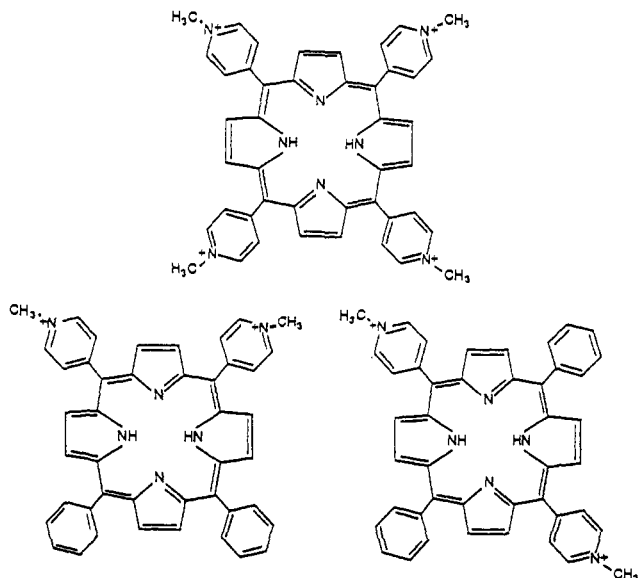


Figure 1. Structures of several water-soluble meso-substituted porphyrins. Upper, tetrakis(*N*-methylpyridinium-4-yl)porphine (H_2T4); lower left, *cis*-bis(*N*-methylpyridinium-4-yl)diphenylporphine (*c*- H_2Pagg); lower right, *trans*-bis(*N*-methylpyridinium-4-yl)diphenylporphine (*t*- H_2Pagg).

porphyrin assembly process. However, instances are known of DNA aggregation which produces no effect on the CD spectrum of the nucleic acid,¹⁸ and, therefore, other methods need be introduced to determine whether, as the proposed model suggests, porphyrin assembly can occur without a requirement for DNA aggregation. In this paper, simple light-scattering measurements of an unusual type are described which address this point. These studies indicate that such resonance light-scattering methods provide an exceedingly sensitive way of detecting extended porphyrin aggregation both alone and on polymer templates.

Experimental Section

The free-base porphyrins used in these studies, tetrakis(*N*-methylpyridinium-4-yl)porphine (H_2T4) and *trans*-bis(*N*-methylpyridinium-4-yl)-diphenylporphine (*t*- H_2Pagg , cf. Figure 1), were obtained from Mid-century as chloride salts. The identity of the substances and extent of peripheral methylation were confirmed by ¹H NMR in DMSO-*d*₆. The porphyrin concentrations were determined in water (no salt added) using $\epsilon = 2.26 \times 10^5$ and $2.40 \times 10^5 \text{ M}^{-1} \text{ cm}^{-1}$ at the respective Soret maxima.^{19,20} The copper(II) and gold(III) derivatives *t*-CuPagg and *t*-AuPagg were synthesized by methods described for similar cationic porphyrins.^{21–23} Molar absorptivities were determined in water (no salt added) using a combination of visible absorption and atomic absorption spectroscopies. The wavelengths and molar absorptivities of the Soret maxima in water are for *t*-CuPagg, 417 nm, $2.34 \times 10^5 \text{ M}^{-1} \text{ cm}^{-1}$, and for *t*-AuPagg, 407 nm, $2.23 \times 10^5 \text{ M}^{-1} \text{ cm}^{-1}$.

Calf thymus (ct) DNA purchased from either Sigma Chemical Co. or Pharmacia was purified using a standard procedure previously described¹¹ and stored in 1 mM phosphate buffer, pH 7, containing 10 mM NaCl. The concentration of DNA was obtained via absorbance measurements using $\epsilon = 1.32 \times 10^4 \text{ M}^{-1} \text{ cm}^{-1}$ at the maximum near 260 nm (i.e., DNA concentrations are reported in molar base pairs).²⁴ The processes considered here are highly cooperative and depend in a sensitive

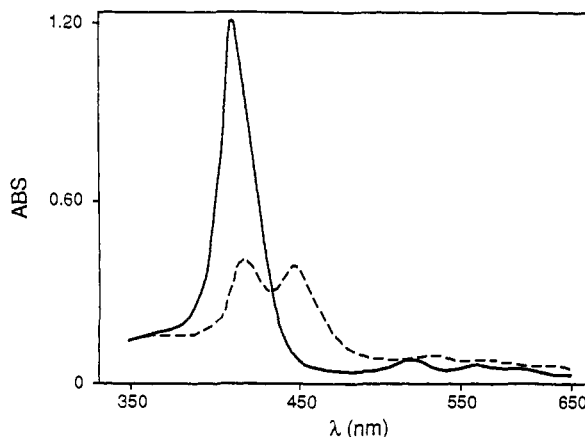


Figure 2. Influence of ionic strength on the absorption spectrum of *t*- H_2Pagg . [*t*- H_2Pagg] = 5 μM , 1 mM phosphate buffer, pH 7. (—) $I = 0.01 \text{ M}$; (---) $I = 0.1 \text{ M}$. NaCl is the added electrolyte.

way on the source of the DNA used. Whereas different lots of DNA produce qualitatively similar results, quantitative details are dependent on the history of the nucleic acid. Studies are underway to determine which factors, including size, are responsible for the variations observed. The spectral experiments reported here were conducted with Sigma Lot No. 67F-9730, and the light-scattering experiments were conducted with Pharmacia DNA Lot BJ4562P03. Another important consideration in the preparation of solutions is the order of mixing reagents. Because several of the studied porphyrins tend to aggregate extensively in water even at moderate salt concentrations, to obtain reproducible results it is necessary to first incubate them with DNA under low salt conditions, where the monomeric form predominates. The last reagent added to the mixture is NaCl, used to adjust the ionic strength to the desired value.

Condensed DNA was prepared by a variation of the method of Widom and Baldwin¹⁸ using Kodak hexaamminecobalt(III) chloride. DNA (40 μM) in 1 mM phosphate buffer, 3 mM NaCl, was made 117 μM in hexaamminecobalt(III). Light-scattering methods (to be described below) were used to confirm that the DNA so treated was in a highly condensed form.

Spectral measurements were performed on Nicolet 9420, Varian 2200, and Aviv 62DS spectrometers. Light-scattering experiments were conducted on a SPEX F111 spectrofluorimeter fitted with a 150-W xenon lamp using right-angle geometry. The excitation and emission monochromator wavelengths were coupled and adjusted to scan simultaneously through the range from 230 to 600 nm.

Results

Even in the *absence of DNA*, addition of NaCl to aqueous solutions of *t*- H_2Pagg or *t*-CuPagg, initially at $I \sim 0$, leads to a large bathochromic shift and hypochromism of the Soret band (Figure 2), indicating extensive aggregation of these porphyrins. In contrast, no significant influence of salt concentration on the spectrum of *t*-AuPagg nor H_2T4 is observed; these porphyrins obey Beer's law over a wide concentration range and, therefore, appear to remain monomeric in aqueous solution even at moderate ($\leq 0.2 \text{ M}$) salt concentrations.²⁵ Very small, conservative CD

(18) Widom, J.; Baldwin, R. L. *J. Mol. Biol.* **1980**, *144*, 431.

(19) Pasternack, R. F.; Huber, P. R.; Boyd, P.; Engasser, G.; Francesconi, L.; Gibbs, E.; Fasella, P.; Cerio Ventura, G.; Hinds, L. *J. Am. Chem. Soc.* **1972**, *94*, 4511.

(20) Sari, M. A.; Battioni, J. P.; Dupre, D.; Mansuy, D.; Le Pecq, J. B. *Biochemistry* **1990**, *29*, 4205.

(21) Pasternack, R. F.; Francesconi, L.; Raff, D.; Spiro, E. *Inorg. Chem.* **1973**, *12*, 2606.

(22) Gibbs, E. J.; Maurer, M. C.; Zhang, J. H.; Reiff, W. M.; Hill, D. T.; Malicka-Blaszkiewicz, M.; McKinnin, R. E.; Liu, H. Q.; Pasternack, R. F. *J. Inorg. Biochem.* **1988**, *32*, 39.

(23) Butze, K.; Nakamoto, K. *Inorg. Chim. Acta* **1990**, *167*, 97.

(24) Pachter, J. A.; Huang, C. H.; Duvernay, V. H.; Prestayko, A. W.; Crooke, S. T.; *Biochemistry* **1982**, *21*, 1541.

(25) Some controversy exists as to the exact nature of H_2T4 in aqueous solution. We have presented a number of spectral and chemical arguments for the monomeric nature of this substance,^{19,26} and recent kinetic²⁷ and optical²⁸ studies concur with this view. However, fluorescence measurements have been interpreted as indicating that H_2T4 exists as a dimer under these conditions,²⁹ and fluorescence lifetime experiments³⁰ are consistent with this dimer model. All authors do agree, however, that if H_2T4 does aggregate in solution, it is limited to dimers under the conditions of these experiments. The aggregation forms of interest to us here are considerably more extended.

(26) Pasternack, R. F.; Gibbs, E. J.; Antebi, A.; Bassner, S.; DePoy, L.; Turner, D. H.; Williams, A.; La Place, F.; Lansard, M. H.; Merienne, C.; Perrée-Fauvet, M.; Gaudemer, A. *J. Am. Chem. Soc.* **1985**, *107*, 8179.

(27) Tabata, M.; Babasaki, M. *Inorg. Chem.* **1992**, *31*, 5268.

(28) Ito, A. S.; Azzellini, G. C.; Silva, S. C.; Serra, O.; Szabo, A. G. *Biophys. Chem.* **1992**, *45*, 79.

(29) Kano, K.; Nakajima, T.; Takei, M.; Hashimoto, S. *Bull. Chem. Soc. Jpn.* **1987**, *60*, 1281.

(30) Liu, Y.; Koningstein, J. A.; Yevdokimov, Y. *Can. J. Chem.* **1991**, *69*, 1791.

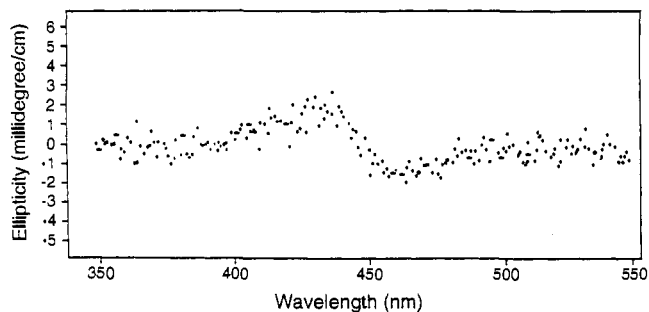


Figure 3. Circular dichroism spectrum of $5 \mu\text{M}$ $t\text{-H}_2\text{Pagg}$ at an ionic strength of 0.1 M , conditions under which the porphyrin is extensively aggregated.

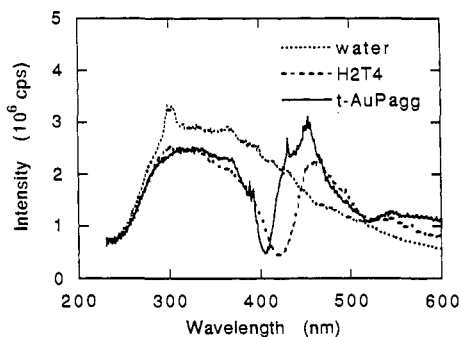


Figure 4. Light-scattering profiles of water, $5 \mu\text{M}$ $\text{H}_2\text{T4}$ at $I = 0.1 \text{ M}$, and $5 \mu\text{M}$ $t\text{-AuPagg}$ at $I = 0.1 \text{ M}$. The minima are at 421 and 404 nm , respectively. The lamp/detector efficiency of the apparatus falls off rapidly as the wavelength decreases below 300 nm .

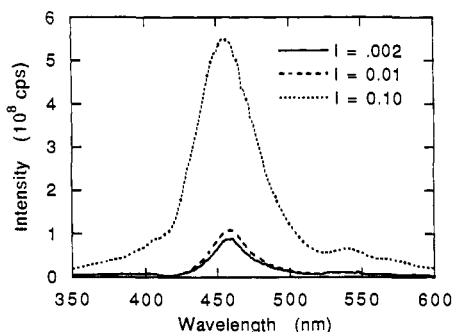


Figure 5. Light-scattering profiles of $5 \mu\text{M}$ $t\text{-H}_2\text{Pagg}$ as a function of ionic strength. The maxima appear at 455 nm .

signals¹³ are obtained for the aggregated porphyrins in the absence of DNA (Figure 3); none at all are observed for $t\text{-AuPagg}$ or $\text{H}_2\text{T4}$.

Light-scattering results are consistent with the conclusions drawn from these experiments as to the state of the solute species. Shown in Figure 4 are the light-scattering profiles for aqueous solutions of $\text{H}_2\text{T4}$ and $t\text{-AuPagg}$ with neat water included for comparison. The presence of the porphyrins has very little impact on the scattering profile except near the Soret maxima, at which photons being absorbed lead to local minima (at 404 nm for $t\text{-AuPagg}$ and 421 nm for $\text{H}_2\text{T4}$). At slightly longer wavelengths there is a characteristic "overshoot" *vis-à-vis* the water base line, but the effect is very small. This pattern can be contrasted with the one obtained for $t\text{-H}_2\text{Pagg}$ or $t\text{-CuPagg}$. As shown in Figure 5, using $t\text{-H}_2\text{Pagg}$ as an example, extensive scattering is obtained for these species, with the scattering profile showing a wavelength dependence characteristic of the absorption spectrum of the scattering species; $\lambda_{\text{max}} \sim 455 \text{ nm}$. The extent of the scattering is dependent on the ionic strength in a manner to be expected for a self-aggregation process involving charged species. The basis for this nonclassical wavelength dependence will be described later, but for now, it should be noted that such resonance light-

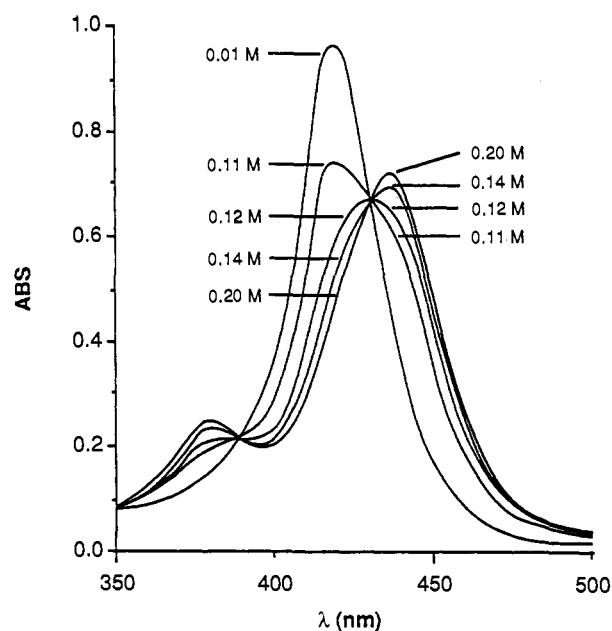


Figure 6. Absorption spectrum in the Soret region of the $t\text{-CuPagg/DNA}$ complex as a function of ionic strength. $[t\text{-CuPagg}] = 5 \mu\text{M}$, $[\text{DNA}] = 70 \mu\text{M}$.

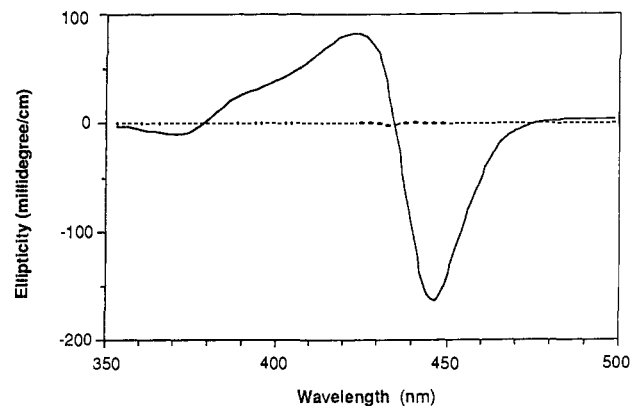


Figure 7. Induced CD spectra for the $t\text{-CuPagg/DNA}$ complex at two ionic strengths, $[t\text{-CuPagg}] = 5 \mu\text{M}$, $[\text{DNA}] = 40 \mu\text{M}$. (---) $I = 0.01 \text{ M}$; (—) $I = 0.17 \text{ M}$.

scattering measurements appear to offer great promise as a sensitive method for detecting extended porphyrin aggregation.

In the presence of DNA, the salt influence on the absorption spectra of the porphyrins is qualitatively similar to that reported in the absence of the nucleic acid—large bathochromic shifts and hypochromicity are observed in the Soret region for $t\text{-H}_2\text{Pagg}$ and $t\text{-CuPagg}$ (Figure 6), but practically no change is seen for $t\text{-AuPagg}$. (Addition of NaCl to $\text{H}_2\text{T4/DNA}$ complexes leads to hypsochromic shifts and hyperchromicity described and interpreted earlier as resulting from a change in binding mode from intercalation to outside, groove binding¹²). The influence of added sodium chloride on the CD signals is even more dramatic. Whereas, from an ionic strength of $0.02\text{--}0.2 \text{ M}$, the induced CD spectrum in the Soret region for $t\text{-AuPagg}$ remains a single, negative feature characteristic of a monodispersed, intercalated porphyrin,^{13,14} significant changes in profile and size of the Soret region CD signals occur for $t\text{-H}_2\text{Pagg}$ and $t\text{-CuPagg}$ over this same ionic strength range. The single, negative induced signal at low ionic strength converts to a bisignate feature 1–2 orders of magnitude larger for these latter porphyrins (Figure 7). Figures 8–10 show the dependence of these induced CD signals on porphyrin, salt, and DNA concentration for $t\text{-H}_2\text{Pagg}$ and $t\text{-CuPagg}$. In all cases, special efforts were made to assure that

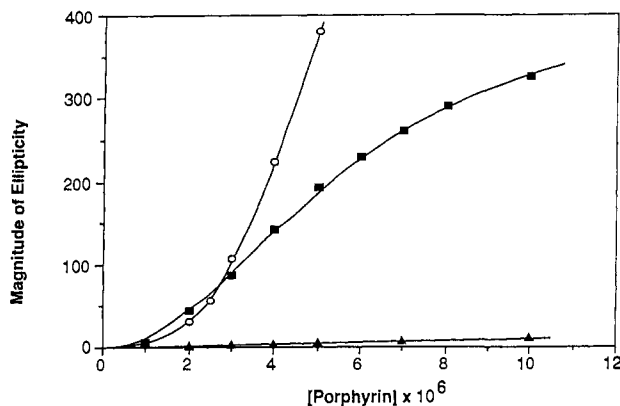


Figure 8. Induced circular dichroism spectra for several porphyrin/DNA complexes as a function of porphyrin concentration. (■) *t*-H₂Pagg at [DNA] = 40 μM, [NaCl] = 0.10 M, λ = 449 nm (negative portion of profile); (○) *t*-CuPagg at [DNA] = 70 μM [NaCl] = 0.17 M, λ = 425 nm (positive part of profile); (▲) *t*-AuPagg at [DNA] = 40 μM, [NaCl] = 0.10 M, λ = 414 nm (at single, negative feature).

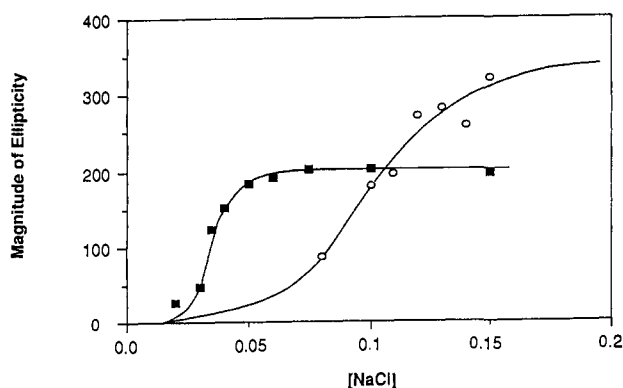


Figure 9. Induced circular dichroism spectra for several porphyrin/DNA complexes as a function of ionic strength (NaCl concentration). (■) 5 μM *t*-H₂Pagg, 40 μM DNA; (○) 5 μM *t*-CuPagg, 70 μM DNA.

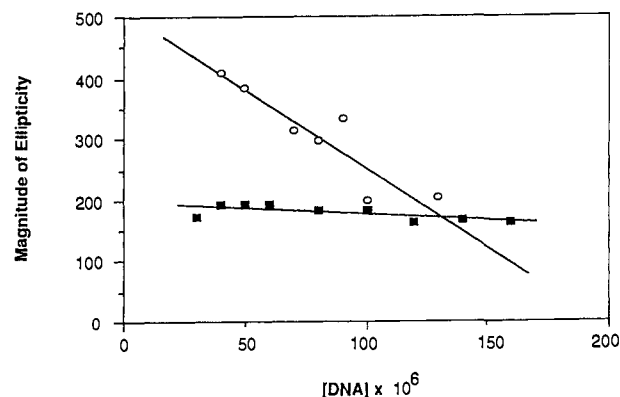


Figure 10. Induced circular dichroism spectra for several porphyrin/DNA complexes as a function of DNA concentration. (■) 5 μM *t*-H₂Pagg, *I* = 0.10 M; (○) 5 μM *t*-CuPagg, *I* = 0.17 M.

the measured signals were equilibrium values.³¹ Defining θ as the magnitude of the ellipticity at some fixed wavelength, the dependence of θ at 414 nm on [*t*-AuPagg] is linear throughout the porphyrin concentration range studied (at [DNA] = 40 μM, [NaCl] = 0.10 M), as would be expected for a monomeric species:

$$\theta_{414} = 1.15 \times 10^6 [t\text{-AuPagg}]$$

However, the θ vs concentration profiles are of a sigmoidal shape

(31) The kinetics of aggregate formation are slow and produce complicated profiles. We are currently analyzing these results and plan to report on them in the near future.

for both *t*-H₂Pagg and *t*-CuPagg, characteristic of a cooperative process, although a nonlinear dependence of optical signals on concentration as a result of excitation delocalization in extended aggregates may also be contributing. Regardless, these profiles are indicative of assembly formation of chromophores, although it is difficult to assess the degree of cooperativity. Empirically derived equations which fit the data satisfactorily are, for *t*-H₂-Pagg,

$$\theta_{449} = \frac{1.33 \times 10^{13} [t\text{-H}_2\text{Pagg}]^2}{1 + 3.05 \times 10^{10} [t\text{-H}_2\text{Pagg}]^2}$$

at [DNA] = 40 μM, [NaCl] = 0.10 M, and for *t*-CuPagg,

$$\theta_{425} = \frac{4.15 \times 10^{18} [t\text{-CuPagg}]^3}{1 + 2.93 \times 10^{15} [t\text{-CuPagg}]^3}$$

at [DNA] = 70 μM, [NaCl] = 0.17 M. These conditions were chosen for *t*-CuPagg to avoid precipitation and to minimize errors from minor variations in ionic strength (see Figure 9). The salt dependencies of θ are also characteristic of cooperative processes and obey equations of the form

$$\theta_{449} = \frac{1.11 \times 10^{13} [\text{NaCl}]^{7.3}}{1 + 5.63 \times 10^{10} [\text{NaCl}]^{7.3}}$$

for [*t*-H₂Pagg] = 5 μM, [DNA] = 40 μM, and

$$\theta_{425} = \frac{4.47 \times 10^7 [\text{NaCl}]^{5.1}}{1 + 1.30 \times 10^5 [\text{NaCl}]^{5.1}}$$

for [*t*-CuPagg] = 5 μM, [DNA] = 70 μM.

The size of the CD signal at equilibrium is much less sensitive to DNA concentration (Figure 10) than other parameters, although it decreases (slightly) with increasing [DNA] over the range studied:

$$\theta_{449} = 211 - 0.324 \times 10^6 [\text{DNA}] \quad \text{and}$$

$$\theta_{425} = 496 - 2.39 \times 10^6 [\text{DNA}]$$

for *t*-H₂Pagg and *t*-CuPagg, respectively. That this dependence is so weak is consistent with our view of the processes as involving assembled porphyrin domains on DNA as the template medium. The form of the equations provided here should serve both as a guide and also as a rigorous test of any theoretical approaches proposed to account for these phenomena and their accompanying optical signals.

Light-scattering measurements are particularly informative as to the nature of the solute species giving rise to the large circular dichroism signals observed here. The scattering profiles for H₂T4/DNA and *t*-AuPagg/DNA which do not provide such anomalous CD signals are qualitatively very similar to those shown in Figure 4, obtained for these porphyrins in the absence of DNA, except that the minima now occur at 427 and 411 nm, respectively, consistent with results from absorption spectroscopy which show bathochromic shifts for these chromophores upon binding to nucleic acids. Both *t*-H₂Pagg and *t*-CuPagg provide very large scattering profiles in the presence of DNA at *I* = 0.1 M (Figure 11), indicating that under these conditions these porphyrins are extensively aggregated. At lower ionic strength (*I* = 0.01 M), the former porphyrin shows much less scattering and the latter, under these conditions, behaves as a nonaggregated species. Indeed, as may be seen in Figure 9, using a CD criterion, at low salt concentrations *t*-CuPagg/DNA complexes are less extensively aggregated than are *t*-H₂Pagg/DNA complexes.

To assess the impact of porphyrin aggregation on the DNA to which it is bound, we conducted light-scattering experiments with

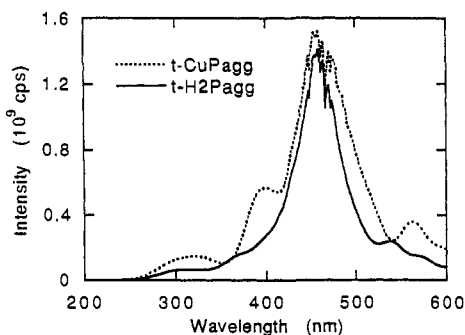


Figure 11. Scattering profiles for *t*-H₂Pagg/DNA and *t*-CuPagg/DNA complexes at an ionic strength of 0.1 M. The porphyrin concentrations are 5 μ M, and the [DNA] is 40 μ M.

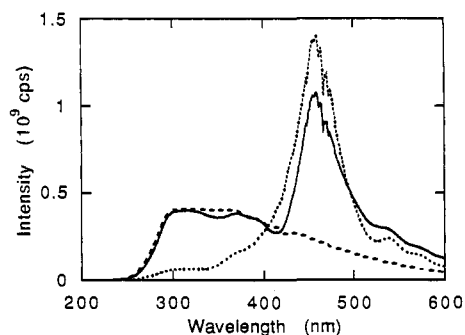


Figure 12. Light-scattering measurements of DNA and DNA/*t*-H₂Pagg complexes. (---) 40 μ M DNA, condensed with hexaamminecobalt(III), 3 mM NaCl; (—) 5 μ M *t*-H₂Pagg, 40 μ M DNA, condensed with hexaamminecobalt(III), 3 mM NaCl; (···) 5 μ M *t*-H₂Pagg, 40 μ M DNA to which no hexaamminecobalt(III) has been added, 0.1 M NaCl. As pointed out earlier, the lamp/detector efficiency of the apparatus falls off rapidly as the wavelength decreases below 300 nm.

both condensed and dispersed nucleic acids. We had previously shown that aggregation of *t*-H₂Pagg or *t*-CuPagg leads to no major impact on the CD spectrum of the DNA to which they are bound; in fact, the CD spectrum in the UV region more closely resembles that of free B-form DNA than do the spectra obtained for intercalator/DNA complexes. However, the absence of an influence on the CD spectrum of DNA does not in itself provide information on the aggregation state of the nucleic acid. Aggregated DNA which provides "normal" CD signals can be obtained, for example, by the addition of hexaamminecobalt(III) to calf thymus DNA *under low salt conditions*. Note that the resultant aggregated DNA scatters light extensively in the UV region (Figure 12). When *t*-H₂Pagg is added to such condensed DNA, a resonance scattering profile is obtained in the visible region which is larger than the one provided at this ionic strength by *t*-H₂Pagg/DNA complexes in the absence of hexaamminecobalt(III); the UV profile due primarily to DNA is almost unaffected, still showing the impact of its being in a condensed state. When these two profiles are compared to the one obtained in the ultraviolet region for a *t*-H₂Pagg/DNA solution at $I = 0.1$ M to which no hexaamminecobalt(III) has been added, it is clear that *the DNA is not extensively aggregated* in this last system, although the porphyrin provides a scattering profile and CD spectrum in the visible range characteristic of a highly aggregated species.

Discussion

The most dramatic effect arising from complexation to nucleic acids by the *t*-H₂Pagg and *t*-CuPagg porphyrin derivatives in the presence of about 0.1 M NaCl is the generation of circular dichroism signals 1–2 orders of magnitude larger than those observed at equivalent concentrations of porphyrin and DNA under low salt conditions. The size of these signals is reminiscent

of the polymer(polypeptide)/salt-induced optical activity signals (Ψ -CD) described in the literature for various DNA aggregates.^{32–34} The usually small CD signals associated with solutions of dispersed nucleic acids became anomalous when the molecules are induced to condense or otherwise form *organized* assemblies. Two types of anomalies of the CD spectra, not observed in unaggregated systems nor for smaller aggregates, occur under such conditions: (i) long tails appear in the CD at wavelengths outside the absorption band of the dispersed molecules and (ii) as the size of the aggregate grows, the magnitude and shape of the CD bands change dramatically.

The theory of Keller and Bustamante³⁵ explains the first type of anomaly (CD tails) as a manifestation of the phenomenon of preferential scattering of the circular polarizations of light due to the long-range chiral structure of the DNA aggregates. Although the second anomaly (the absorption Ψ -type CD) is also a manifestation of the long-range chiral structure of the aggregates, it has a different physical origin. When DNA molecules are in a *dispersed* state, the electronic excitations created at a given point in the molecule remain localized and the interactions between adjacent chromophores (DNA bases in this case) do not extend more than a few angstroms away from the excitation site. The molecule reacts to the incident light as a collection of localized excitations, and the circular polarizations probe the short-range chirality of the molecule. In contrast, in large, dense, chiral DNA molecular aggregates, the excitation can be delocalized throughout the entire particle. The extent of the delocalization depends in turn on the strength of the coupling among chromophores. This coupling is determined by the extinction coefficient of the isolated chromophores, their density in the aggregate, their spatial relationships in space, their spatial extension, the dimensionality of the aggregates, and the degree to which the long-range chirality of the aggregate matches the wavelength of the incident light. When the requirements for delocalization are met, the aggregate reacts as a single entity via a series of *collective* modes of excitation; the delocalization can extend to dimensions comparable to the size of the whole aggregate. If the packing of the aggregate is chiral, certain collective modes can be preferentially excited by one circular polarization over the other, giving rise to preferential absorption (CD) signals.

Generally, three-dimensional aggregates are able to delocalize the excitation more efficiently than two-dimensional (membrane) or one-dimensional (chain-like) systems, because on the average, in a three-dimensional aggregate, each chromophore is surrounded by a larger number of neighbors with which it can interact and delocalize the energy. In practice, however, the different factors can offset and/or compensate one another. For example, aggregates with a low chromophore density can still display strong delocalization if the individual chromophores possess large extinction coefficients. This is because the chromophore interaction and therefore the efficiency of delocalization is proportional roughly to the square of the extinction coefficient of the chromophores. Similarly, a highly structured, quasicrystalline chromophore organization can compensate for a low extinction coefficient of the chromophore or a somewhat smaller size of the aggregate. An interesting example of this compensation is provided by condensates of DNA-dye complexes.^{36,37} In these previous investigations, the DNA condensates were prepared having strongly absorbing dyes *intercalated* between the bases.

(32) Carrol, D. *Biochemistry* **1972**, *11*, 421.

(33) Shaprio, J. T.; Leng, M.; Felsenfeld, G. *Biochemistry* **1969**, *8*, 3219.

(34) Haynes, M.; Garrett, R. A.; Gratzner, W. B. *Biochemistry* **1970**, *9*, 4410.

(35) Keller, D.; Bustamante, C. *J. Chem. Phys.* **1986**, *84*, 2972.

(36) Phillips, C. L.; Mickols, W. E.; Maestre, M. F.; Tinoco, I., Jr. *Biochemistry* **1986**, *25*, 7803.

(37) (a) Bustamante, C.; Samori, B.; Builes, E. *Biochemistry* **1991**, *30*, 5661. (b) Yevdokimov, Y. M.; Salyanov, V. I.; Dembo, A. T.; Berg, H. *Biomed. Biochem. Acta* **1983**, *42*, 855.

In these cases, in addition to the Ψ -type CD spectrum due to the DNA moiety, a subsidiary Ψ -type CD was observed at the absorption band of the chromophores. It was found that such effects can be obtained at relatively low fraction of bound dye molecules if they are bound to the densely packed, chiral assembly. Presumably, then, in this instance, the three-dimensional delocalization throughout the whole aggregate suffices to produce large CD signals even without a high chromophore density.

The above discussion suggests, then, that for the systems considered here a conjunction of two effects—high values of the oscillator strengths of the porphyrin dyes (integrated absorption coefficient $> 10^{18} \text{ mol}^{-1} \text{ m}^2 \text{ s}^{-1}$, $f \sim 2$) and arrangement of the porphyrins into a quasicrystallite involving a high linear density of dyes on the DNA surface—might lead to a very efficient excitation delocalization mechanism able to operate in what appears to be a one-dimensional system. The cooperativity in the surface binding of the porphyrins to DNA described earlier will naturally result in such a high linear density of the dyes, thereby contributing to an efficient delocalization of the excitation.

Of interest when comparing the earlier results on DNA-dye condensates to those described here is the observation that the CD signals of the intercalated dyes are monosignate, implying that any short-range excitonic delocalization is being masked and dominated by long-range interactions. *Of even greater significance is the fact that the DNA to which the porphyrins are bound in the present study is not extensively aggregated, as evidenced by light-scattering results.*

Although it is well-known that light-scattering experiments provide extremely useful information concerning particle size and shape, measurements have typically been made at wavelengths away from absorption bands. What has apparently not been generally appreciated by workers in the field is that light-scattering at wavelengths in the absorption band envelope—a form of resonance light-scattering—can be considerable if the absorption is not too strong and the particle size is sufficiently large. Under these conditions, such experiments can be very useful in providing information on the extent of aggregation of molecules containing chromophores.

The theoretical ideas necessary for understanding resonance light-scattering from aggregates can take two forms. The aggregate can be viewed as a collection of polarizable molecules or as a particle with an index of refraction different from that of the surrounding medium. The latter lends itself to a simple discussion, so we include it here.

The extent to which a particle absorbs and scatters light depends on its size, shape, and index of refraction relative to the surrounding medium (both real and imaginary parts). In fact, if the size of a spherical particle is much less than the wavelength of light in the surrounding medium and if the refractive index of the sphere divided by the refractive index of the surrounding medium, $m = n_{\text{sph}}/n_{\text{med}}$, is not too large, the calculation is simplified; this effect is widely referred to as Rayleigh scattering. If r is the radius of the sphere and λ is the free-space wavelength, then the cross sections for absorption and scattering are³⁸

$$c_{\text{abs}} = (\pi r^2) 4x \text{Im}\{(m^2 - 1)/(m^2 + 2)\} \text{ and}$$

$$c_{\text{sca}} = (\pi r^2) (\frac{8}{3}) x^4 \{(m^2 - 1)/(m^2 + 2)\}^2$$

where x is the size parameter and equals $(2\pi r n_{\text{med}})/\lambda$. In a region near a spectral maximum, the real part of m varies and the imaginary part of m increases, causing not only the absorption but also the scattering cross section to increase. The important point to note is that although the absorption and scattering cross sections both depend on both the real and imaginary parts of m , the scattering is a much stronger function of m than the absorption cross section. Therefore, under certain conditions, enhanced

scattering at wavelengths in the absorption band will be observed in spite of the increase in photon absorption. Accordingly, whereas the experimental profiles shown in Figure 4 for nonaggregating porphyrins show a minimum at the wavelength of maximum absorption, the profiles in Figure 5 for the aggregated *t*-H₂Pagg show enhanced scattering in this region.

Scattering experiments typically measure the photon flux at some angle or range of angles using either polarized or unpolarized incident light. The exact arrangement and type of light source and detector are therefore important in determining the amount of scattering which is measured. Once these conditions are fixed, however, the amount of scattered light detected is proportional to the scattering cross section (reduced by the amount of absorption and scattering in the sample). If the cross section for scattering is a stronger function of m than the cross section for absorption and if the concentration is low enough that absorption and scattering in the sample are not too large, then enhanced scattering is observed.

The reason that this technique of resonance light-scattering is so useful for aggregation experiments is that absorption and scattering depend on the size of the aggregate in very different ways. Imagine the case in which a *fixed concentration* of material is under study. The absorption due to each sphere is proportional to the volume of the sphere, but the number of spheres per unit volume is inversely related to the volume of the sphere. The amount of absorption is therefore independent of the size of spheres. This is implied by the Beer-Lambert law since the absorption for a fixed path length should depend on the concentration of the material in the sample and nothing else. On the other hand, the scattering due to each sphere is proportional to the square of the volume. Since the number density of spheres depends inversely on the volume, the amount of scattering is *directly proportional* to the volume of each sphere. Thus, the larger the aggregate, the greater the scattering.

To relate these ideas to our experiment, we calculate the amount of absorption and scattering for *t*-H₂Pagg bound to DNA, using a simple model. First, we make the assumption (to be relaxed later) that the *t*-H₂Pagg aggregates can be considered as spheres. Second, we assume that the absorption is due to a collection of identical, independent, isotropic, damped, harmonic oscillators with a resonant wavelength of about 450 nm (Lorentz model).³⁹ We then adjust the density of oscillators and the damping factor so that a 5.2 μM solution of chromophores produces an absorption band roughly 20 nM wide with a peak absorbance of about 0.5 for a 1-cm path length, approximately the experimental result for *t*-H₂Pagg. The maximum value for the imaginary part of the relative index of refraction turns out to be about 0.8, and as noted earlier, the radius of the spheres does not affect the absorption spectrum. To see the results of this model, the absorption and scattering cross sections of 10-Å-radius spheres for three different densities of oscillators S are shown in Figure 13. In order to simulate experimental conditions, the radius of the spheres was varied (keeping the concentration constant), and absorption and scattering in the 1-cm cuvette both before and after the scattering event were taken into account. The results are shown in Figure 14, where the independence of the absorption on sphere radius and the strong dependence of the scattering on sphere radius are evident. Notice that the scattering peak is significantly decreased and altered in shape by the absorption and scattering in the cuvette and that the scattering peak is wider than the absorption peak, as is found for both *t*-H₂Pagg and *t*-CuPagg.

Several ideas are worth noting. First, Rayleigh scattering depends on the inverse fourth power of wavelength ($c_{\text{sca}} \approx x^4$), but only if m does not vary with wavelength. Experiments to check this wavelength dependence must therefore be conducted away from absorption bands. In our experiments, the dependence

(38) Bohren, C. F.; Huffman, D. R. *Absorption and Scattering of Light by Small Particles*; John Wiley and Sons: New York, 1983; p 135.

(39) Bohren, C. F.; Huffman, D. R. *Absorption and Scattering of Light by Small Particles*; John Wiley and Sons: New York, 1983; p 228.

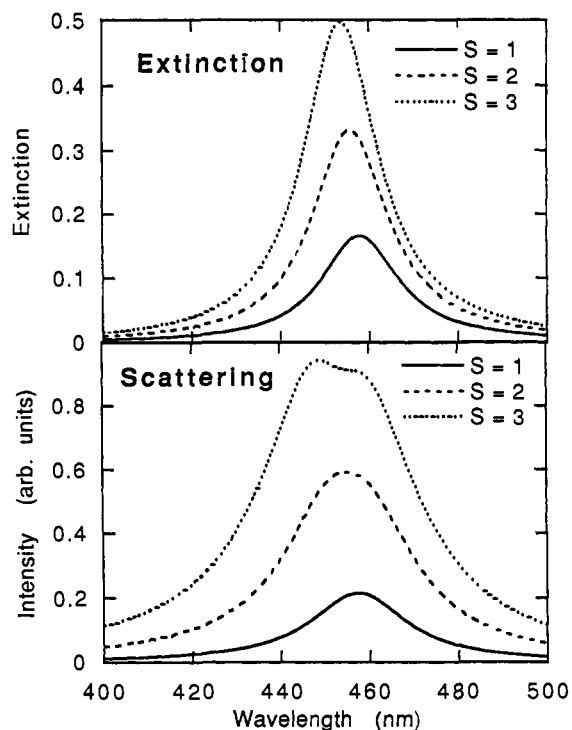


Figure 13. Calculated extinction and scattering cross sections for 10-Å-radius spheres with three different densities of oscillators, S (the units are arbitrary). Extinction equals $-\log T$ and includes contributions from both absorbance and scattering.

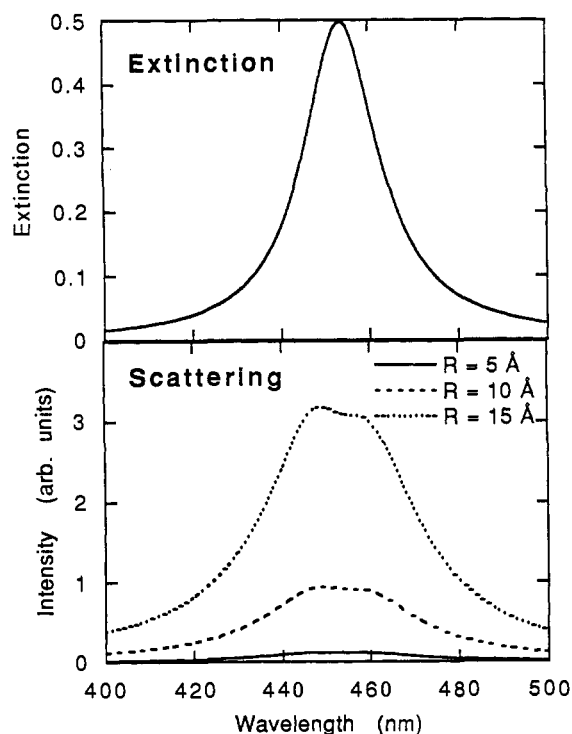


Figure 14. Calculated extinction and scattering spectra for one density of oscillators ($S = 3$) and three different radii of spheres. The scattering spectrum has been reduced and altered in shape by absorption and scattering in the sample. Extinction is as defined for Figure 13.

of the scattering on wavelength inside the absorption band is due almost entirely to changes in m and only less so to changes in wavelength. Second, it is clearly a gross simplification to view

the t -H₂Pagg aggregates on DNA as spheres. In fact, as long as (1) the wavelength is much greater than the dimensions of nonspherical particles and (2) the orientation of the nonspherical particles is randomly distributed in the medium (i.e., the t -H₂Pagg/DNA complexes are not ordered in the sample), the absorption and scattering cross sections are only weakly dependent on shape. For example, if our calculations are repeated for ellipsoids rather than spheres, the absorption and scattering results are qualitatively the same and quantitatively changed by less than 10% for ellipsoids with a 10:1 length-to-width ratio.

In the experiments described here, it was shown that DNA, condensed with hexaamminecobalt(III), provides a light-scattering signal in the UV region some 2 orders of magnitude larger than that for nonaggregated DNA at the same concentration. Although the condensed nucleic acid light-scattering profile, unlike those obtained for porphyrin aggregates, does not show a pronounced maximum near its λ_{\max} (at 260 nm), there are likely a number of factors contributing to this difference in scattering profile involving, for example, differences in absorption characteristics for the two species (DNA has a much smaller molar absorptivity than do porphyrins) and their dimensions and packing characteristics, as well as instrumental limitations.

Addition of t -H₂Pagg to aggregated DNA has little effect on the scattering profile in the ultraviolet region (the signal remains about 2 orders of magnitude larger than that observed for dispersed DNA), but, in addition, a large resonance scattering signal is observed in the visible range, near the λ_{\max} for aggregated t -H₂Pagg. However, when t -H₂Pagg is added to *uncondensed* DNA, the scattering profile in the UV region is markedly diminished and differs in shape: t -H₂Pagg alone does not appear to promote DNA aggregation. This is in spite of the fact that the porphyrin itself is clearly in an aggregated state and provides circular dichroism signals characteristic of its being bound to DNA. These results are consistent with the model proposed by us in which unaggregated DNA can serve as a (template) backbone on which t -H₂Pagg and t -CuPagg form long-range chiral assemblies.

The relatively high ionic strengths required to induce the large-type CD signals observed in the present studies suggest that these porphyrins, when intercalated in nonaggregated DNA, have neither the surface density nor the electronic interaction required for Ψ -type effects in linear systems. Raising the ionic strength promotes surface binding (and aggregation of the porphyrins on the DNA surface), which gives rise to anomalous bisignate CD signals as the porphyrins are brought into closer contact, increasing their linear chromophore density and the strength of their electronic interaction.

An important factor in the characterization of these assemblies that requires investigation is a determination of the minimum size of the array of porphyrin molecules required to give rise to these large anomalous signals. This question can be addressed in principle through systematic studies with a variety of DNA restriction fragments of well-defined length. Such studies are now underway. Also, whereas the available evidence appears to support the model, we have proposed (that the porphyrins are arranged on the outside of the helical DNA (or polypeptide¹⁶) molecule following the template's periodicity), we cannot completely rule out at this point the possibility that the porphyrins organize in a larger (higher dimensional) chiral periodic array commensurate with the biopolymer helix.

Acknowledgment. We gratefully acknowledge the support of the National Science Foundation (CHEM-8915264 and DMR-9196048) and the Consiglio Nazionale Delle Ricerche.